Superfluid vortex reconnections at non-zero temperatures

P. Z. Stasiak, A. Baggaley, and C.F. Barenghi
School of Mathematics, Statistics and Physics, Newcastle University, Newcastle upon Tyne, NE1 7RU, United Kingdom

G. Krstulovic
Université Côte d'Azur, Observatoire de la Côte d'Azur, CNRS,Laboratoire Lagrangre, Boulevard de l'Observatoire CS 34229 - F 06304 NICE Cedex 4, France

L. Galantucci
Istituto per le Applicazioni del Calcolo "M. Picone" IAC CNR, Via dei Taurini 19, 00185 Roma, Italy
(Dated: September 18, 2024)

Introduction.— Reconnections are the fundamental events that change the topology of the field lines in fluids and plasmas during their time evolution. Reconnections thus determine important physical properties, such as mixing and inter-scale energy transfer in fluids, or solar flares and tokamak instabilities in plasmas [1]. The nature of reconnections is more clearly studied if the field lines are concentrated in well-separated filamentary structures: vortices in fluids and magnetic flux tubes in plasmas. In superfluid helium this concentration is extreme, providing an ideal context: superfluid vorticity is confined to vortex lines of atomic thickness (approximately $a_0 \approx 10^{-10}$ m); a further simplification is that, unlike what happens in ordinary fluids, the circulation of a superfluid vortex is constrained to the quantised value $\kappa = h/m = 9.97 \times 10^{-8}$ m^2/s, where m is the mass of one helium atom and h is Planck's constant.

It was in the superfluid context that it was theoretically and experimentally recognized [2–7] that reconnections share a universal property irrespective of the initial condition: the minimum distance between reconnecting vortices, δ, scales with time, t, according to the form

$$\delta^{\pm}(t) = A^{\pm}(\kappa|t-t_0|)^{1/2}, \tag{1}$$

where t_0 is the reconnection time, and the dimensionless prefactors A^- and A^+ refer respectively to before ($t < t_0$) and after ($t > t_0$) the reconnection. The same scaling law was then found for reconnections in ordinary viscous fluids [8]. In the case of a pure superfluid at temperature $T = 0$, theoretical work based on the Gross-Pitaevskki equation (GPE) has shown that $A^+ > A^-$, that is, after the reconnection, vortex lines move away from each others faster than in the initial approach; this result has been related to irreversibility [9], and is caused by a rarefaction pulse created immediately after the reconnection[5, 10] which removes some of the kinetic energy of the vortex configuration. This acoustic energy loss depends on the ratio A^+/A^-, which in turns depends on the angle of collision between the vortices [9].

However most helium experiments are performed at temperatures $T > 1$ K, a regime in which thermal excitations form a fluid called the *normal fluid* which provides a viscous route to irreversibility. The aim of this Letter is to investigate finite-temperature effects on vortex reconnections. To achieve this aim we need a more powerful model than the GPE to account not only for the dynamics of the superfluid vortices, but also for the dynamics of the normal fluid. We shall show that at non-zero temperatures Eq. 1 and the relation $A^+ > A-$ hold true, in agreement with experiments. Finally we shall show that, when applied to a turbulent superfluid, a vortex reconnection is a punctuated energy injection into the normal fluid. When applied to turbulence, this last result implies that if the vortex line density (hence the frequency of reconnections) is large enough, vortex reconnections can maintain the normal fluid in a perturbed state.

Method.— We follow the approach of Schwarz [11] which exploits the vast separation of length scales between the vortex core a_0 and any other relevant distance, in particular the average distance between vortices, ℓ, in the case of turbulence. Vortex lines are described as space curves $\mathbf{s}(\xi, t)$ where ξ is arclength. The equation of motion of the vortex lines is

$$\dot{\mathbf{s}}(\xi,t) = \mathbf{v}_s + \frac{\beta}{(1+\beta)}\left[\mathbf{v}_{ns}\cdot\mathbf{s}'\right]\mathbf{s}' + \beta\mathbf{s}'\times\mathbf{v}_{ns} + \beta'\mathbf{s}'\times\left[\mathbf{s}'\times\mathbf{v}_{ns}\right], \tag{2}$$

where $\dot{\mathbf{s}} = \partial\mathbf{s}/\partial t$, $\mathbf{s}' = \partial\mathbf{s}/\partial\xi$ is the unit tangent vector, $\mathbf{v}_{ns} = \mathbf{v}_n - \mathbf{v}_s$, $\mathbf{v}_n$ and $\mathbf{v}_s$ are the normal fluid and superfluid velocities at $\mathbf{s}$, and β, β' are temperature and Reynolds number dependent mutual friction coefficients [12]. The superfluid velocity $\mathbf{v}_s$ at a point $\mathbf{x}$ is determined by the Biot-Savart law

$$\mathbf{v}_s(\mathbf{x},t) = \frac{\kappa}{4\pi}\oint_{\mathcal{T}} \frac{\mathbf{s}'(\xi,t)\times[\mathbf{x}-\mathbf{s}(\xi,t)]}{|\mathbf{x}-\mathbf{s}(\xi,t)|}d\xi, \tag{3}$$

where $\mathcal{T}$ denotes the entire vortex configuration. Superfluid vortices are coupled to a classical description of the incompressible ($\nabla\cdot\mathbf{v}_n = 0$) normal fluid via the mutual friction force $\mathbf{F}_{ns}$

$$\frac{\partial\mathbf{v}_n}{\partial t} + (\mathbf{v}_n\cdot\nabla)\mathbf{v}_n = -\frac{1}{\rho}\nabla p + \nu_n\nabla^2\mathbf{v}_n + \frac{\mathbf{F}_{ns}}{\rho_n}, \tag{4}$$

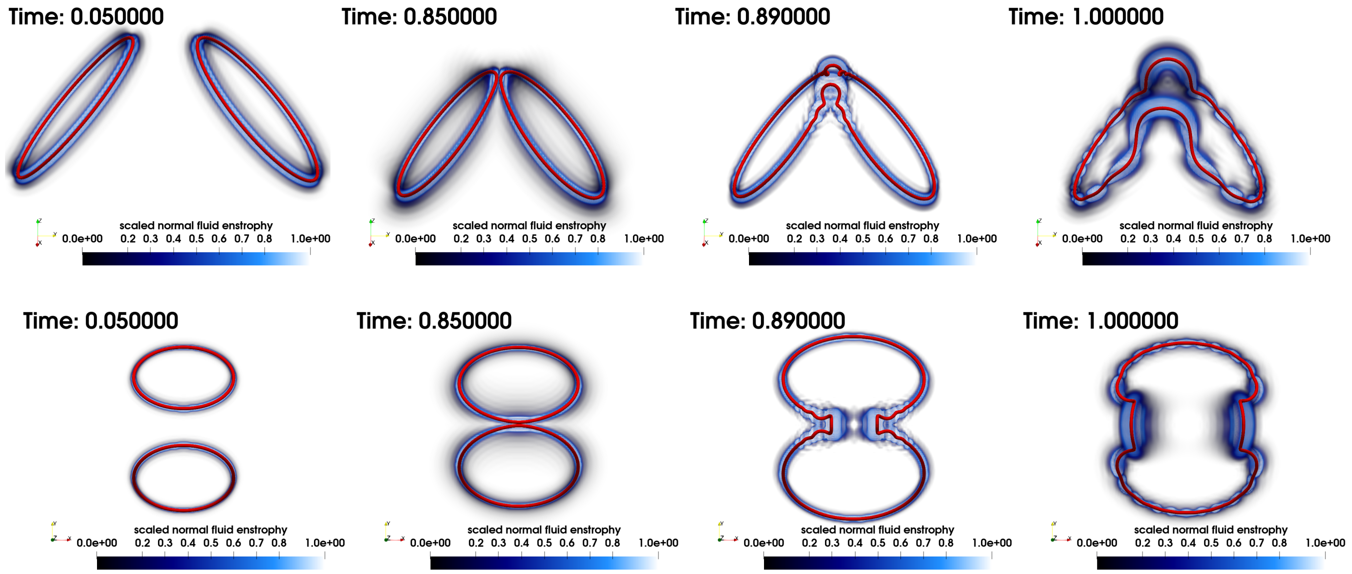

FIG. 1: 3D rendering of vortex ring collisions, from a tent-like initial condition. The red tube represents a superfluid vortex, where the radius has been greatly exaggerated for visual purposes, and the blue volume rendering represents the scaled normal fluid enstrophy $\boldsymbol{\omega}^2/\boldsymbol{\omega}_{max}^2$. *Top row:* Isometric view. *Bottom row:* View of the xy-plane.

where $\rho = \rho_n + \rho_s$ is the total density, ρ_n and ρ_s are the normal fluid and superfluid densities, p is the pressure, and ν_n is the kinematic viscosity of the normal fluid.

Initial configurations.— We consider two distinct initial vortex configurations at $T = 0K, 1.9K$ and $2.1K$. The first is a Hopf link, which consists of two linked rings of radius $R \approx 1$ with an offset in the xy-plane defined by parameters Δl_x and Δl_y. The offsets are chosen so that $(\Delta l_x, \Delta l_y) \in \{(0.125i, 0.125j)|i,j = -3, \cdots, 3\}$, providing us with a total of 49 reconnections for each temperature. The second configuration is of two vortex rings of radius $R \approx 1$ in a tent-like shape (see Fig. 1), making the angle α with the vertical direction. We take 12 realisations of α, such that $\alpha \in \{i\pi/13|i = 1, \cdots, 12\}$. The supplementary material gives more details of our model and these configurations [13]. In all cases, normal fluid structures in the form of rings are initially superimposed to match the vortex lines, eliminating the transient phase of generating these normal fluid structures.

Results.— In the case of the Hopf link the interaction between the two rings leads to a reconnection. We have performed 147 simulations (49 across 3 temperatures) as shown in Fig. 2a and verified Eq. 1 for the minium distance δ. The prefactors $A^{\pm}$ have been computed in the shaded region of the figure. In the pre-reconnection regime we observe a clear segregation of the values of A^- due to temperature. In stark contrast, there is no memory of the temperature in the post-reconnection regime.

HERE Interestingly, the A^+ distribution does not drastically change when including finite temperature effects, suggesting a minor role of the normal fluid in the reconnection dynamics. Our results confirm the irreversibility of vortex reconnections in our finite temperature model, for which $A^+ \geq A^-$. As shown in Fig. 2b, the $T = 0K$ calculation for helium is in good agreement with the Gross-Pitaevskii (GP) model where $A^- \sim 0.4$-0.6, for both initial conditions. Recent investigation in the classical Navier-Stokes [8] have displayed a clear 1/2 power law scaling and pre-factor ratio $A^- \sim 0.3$-0.4, which again shows good agreement with the results that we have presented here for finite temperature.

The steep energy injection observed at reconnection time in the normal fluid kinetic energy E_n is driven by the violent topological change in the vortex geometry. The coupling mutual fricition force $\mathbf{f}_{ns}(\mathbf{s})$, in the first approximation $|\mathbf{f}_{ns}| \propto |\dot{\mathbf{s}} - \mathbf{v}_n| \propto \zeta$, where $\zeta = |\mathbf{s}''|$ is the curvature of the vortex line at $\mathbf{s}$. The curvature ζ spikes when the post-reconnection cusp is created, viciously stirring the normal fluid and generating excitations [14], see Fig. 1. The prefactor ratio A^+/A^- has been shown in recent literature [6, 9, 15] to be of importance in describing fundamental properties of reconnections using the Gross-Pitaevskii (GP) equation. Due to the *ad-hoc* nature of vortex recnnections in our helium model, it is not trivial to derive a linear theory in the limit $\delta^{\pm} \to 0$.

The total energy injected into the normal fluid by the reconnection ΔE_n, which we refer to as energy jumps, is computed by

$$\Delta E_n = \max\left[E_n(t > t_0)\right] - E_n^0 \qquad (5)$$

where E_n^0 is the normal fluid kinetic energy at reconnection time $E_n^0 = E_n(t_0)$. The normalised energy jumps are shown in Fig. 4, plotted against the prefactor ratio A^+/A^-. Here, we observe that a higher value of A^+/A^-,

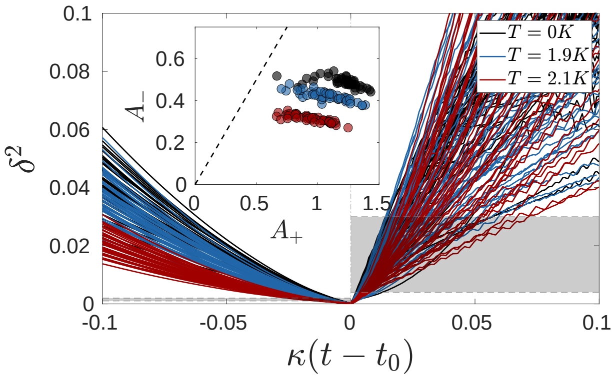

(a)

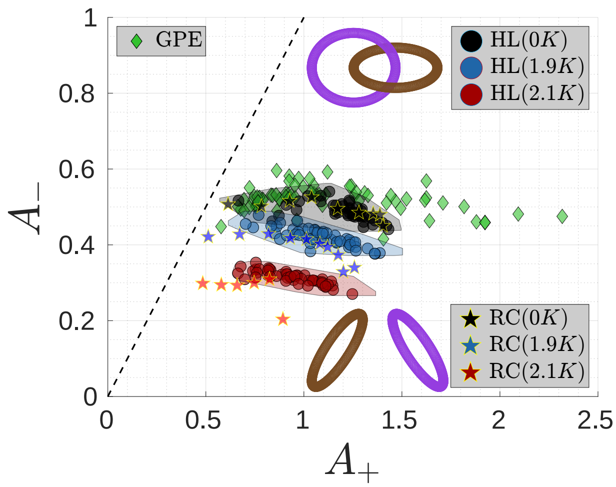

(b)

FIG. 2: *(a)*: Time evolution of the minimum distance squared δ^2 for the Hopf link initial conditions at $T = 0K, 1.9K$ and $2.1K$. The grey shaded area represens the vertical region used to estimate the prefactors $A^{\pm}$. *Inset:* Values of the seperation prefactor A^+ and approach prefactors A^-. *(b)*: Comparison of all prefactor values, *HL*-Hopf link (circles), *RC*-ring collision (stars with yellow outline), GPE-data from Gross-Pitaevskii simulations from Villois *et al.* [9]. The shaded areas associated with each colour represent the convex hull of errors for each temperature.

i.e a larger asymmetry in reconnection dynamics, in fact leads to smaller normal fluid excitations during the reconnection procedure. The emission of sound pulses is a common feature of superfluid vortex reconnections [10] which is restricted by our incompressible hydrodynamic model. In the local induction approximation, the superfluid kinetic energy is proportional to the length of filaments $E_s \propto L$. To compensate for this expulsion of superfluid kinetic energy, a portion of line length ΔL is removed during reconnection. At $T = 0K$, the absence of a dissipative normal fluid removes any possible sinks of energy, and so ensures that any removal of en-

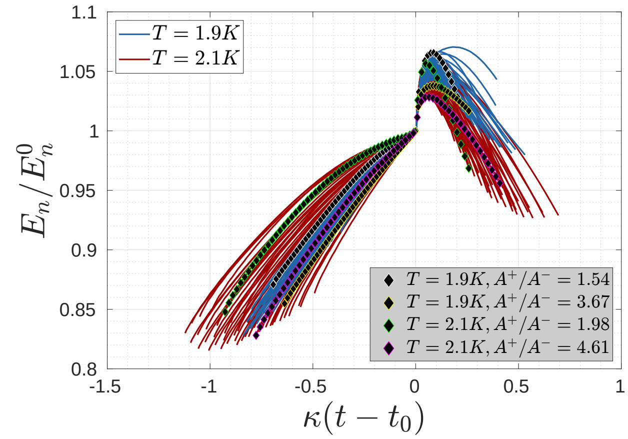

FIG. 3: Total normal fluid kinetic energy E_n scaled by the kinetic energy at reconnection time E_n^0. Black diamonds represent the simulations with minimum and maximum prefactor ratios A^+/A^- at $T = 1.9K$ and $T = 2.1K$ respectively.

ergy $\Delta E_s \propto \Delta L$. Consequentially, as shown as black diamonds in Fig. 4, the superfluid energy E_s that would be transferred to a sound pulse, $-\Delta L/L_0$, exhibits the same characteristic behaviour as the normal fluid energy injected $\Delta E_n/E_n^0$. Remarkably, the theoretical sound pulse energy $-\Delta L/L_0$ at $T = 0K$ is in very good agreement with the energy pulse generated in the GP.

A fully developed turbulent tangle of vortices [16] can be characterised by the vortex line density $\mathcal{L}$, where the frequency of vortex reconnections f is given by $f = (\kappa/6\pi)\mathcal{L}^{5/2}\ln(\mathcal{L}^{-1/2}/a_0)$. From Fig. 3 we can define the normal fluid reconnection relaxation time τ_n, to be the time after reconnection at which the normal fluid energy E_n/E_0 decays by viscosity to the pre-reconnection level. Using this timescale, we estimate the average vortex line density that is required to sustain the normal fluid in a turbulent state via frequent vortex reconnections to be $\mathcal{L} \sim 8 \times 10^7 \mathrm{m}^{-2}$. Experiments in helium-4 [17–20] and in helium-3 [21] are capable of reaching a vortex line density several orders of magnitude larger than the estimated value to sustain a turbulent normal fluid state.

Closing remarks.—

[1] I. T. Chapman, R. Scannell, W. A. Cooper, J. P. Graves, R. J. Hastie, G. Naylor, and A. Zocco, Magnetic Reconnection Triggering Magnetohydrodynamic Instabilities during a Sawtooth Crash in a Tokamak Plasma, Phys. Rev. Lett. **105**, 255002 (2010).

[2] S. Nazarenko and R. West, Analytical Solution for Nonlinear Schrödinger Vortex Reconnection, Journal of Low Temperature Physics **132**, 1 (2003).

[3] G. P. Bewley, M. S. Paoletti, K. R. Sreenivasan, and

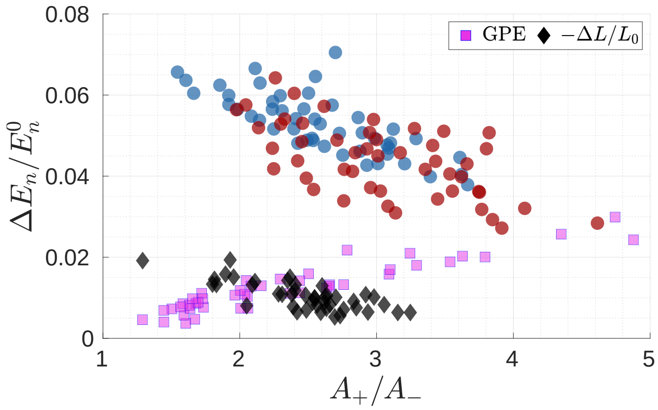

FIG. 4: The total energy jump ΔE_n, the increase in normal fluid kinetic energy due to a superfluid vortex reconnection, for the Hopf links. The solid black diamond represents the change in line length ΔL in the $T = 0K$ case, and the purple squares are from GP simulations from Villois *et al.* [9]

D. P. Lathrop, Characterization of reconnecting vortices in superfluid helium, Proc. Natl. Acad. Sci. **105**, 13707 (2008).

[4] M. S. Paoletti, M. E. Fisher, and D. P. Lathrop, Reconnection dynamics for quantized vortices, Physica D: Nonlinear Phenomena **239**, 1367 (2010).

[5] S. Zuccher, M. Caliari, A. W. Baggaley, and C. F. Barenghi, Quantum vortex reconnections, Physics of Fluids **24**, 125108 (2012).

[6] A. Villois, D. Proment, and G. Krstulovic, Universal and nonuniversal aspects of vortex reconnections in superfluids, Phys. Rev. Fluids **2**, 044701 (2017).

[7] L. Galantucci, A. W. Baggaley, N. G. Parker, and C. F. Barenghi, Crossover from interaction to driven regimes in quantum vortex reconnections, Proc Natl Acad Sci USA **116**, 12204 (2019).

[8] J. Yao and F. Hussain, Separation scaling for viscous vortex reconnection, J. Fluid Mech. **900**, R4 (2020).

[9] A. Villois, D. Proment, and G. Krstulovic, Irreversible Dynamics of Vortex Reconnections in Quantum Fluids, Phys. Rev. Lett. **125**, 164501 (2020).

[10] M. Leadbeater, T. Winiecki, D. C. Samuels, C. F. Barenghi, and C. S. Adams, Sound Emission due to Superfluid Vortex Reconnections, Phys. Rev. Lett. **86**, 1410 (2001).

[11] KW. Schwarz, Three-dimensional vortex dynamics in superfluid ^{4}He, Phys. Rev. B **38**, 2398 (1988).

[12] L. Galantucci, A. W. Baggaley, C. F. Barenghi, and G. Krstulovic, A new self-consistent approach of quantum turbulence in superfluid helium, Eur. Phys. J. Plus **135**, 547 (2020).

[13] See Supplementary Materials at ....

[14] P. Z. Stasiak, A. W. Baggaley, G. Krstulovic, C. F. Barenghi, and L. Galantucci, Cross-Component Energy Transfer in Superfluid Helium-4, J. Low Temp. Phys. (2024).

[15] D. Proment and G. Krstulovic, Matching theory to characterize sound emission during vortex reconnection in quantum fluids, Phys. Rev. Fluids **5**, 104701 (2020).

[16] C. F. Barenghi and D. C. Samuels, Scaling Laws of Vortex Reconnections, Journal of Low Temperature Physics **136**, 281 (2004).

[17] K. W. Schwarz and C. W. Smith, Pulsed-ion study of ultrasonically generated turbulence in superfluid 4He, Physics Letters A **82**, 251 (1981).

[18] F. P. Milliken, K. W. Schwarz, and C. W. Smith, Free Decay of Superfluid Turbulence, Phys. Rev. Lett. **48**, 1204 (1982).

[19] P.-E. Roche and C. F. Barenghi, Vortex spectrum in superfluid turbulence: Interpretation of a recent experiment, EPL **81**, 36002 (2008).

[20] P.-E. Roche, P. Diribarne, T. Didelot, O. Français, L. Rousseau, and H. Willaime, Vortex density spectrum of quantum turbulence, EPL **77**, 66002 (2007).

[21] D. I. Bradley, D. O. Clubb, S. N. Fisher, A. M. Guénault, R. P. Haley, C. J. Matthews, G. R. Pickett, V. Tsepelin, and K. Zaki, Decay of Pure Quantum Turbulence in Superfluid ^{3}He-B, Phys. Rev. Lett. **96**, 035301 (2006).